

## Development of Pd-immobilized porous polymer catalysts via Bayesian optimization

Zhou, Xincheng

Department of Chemical Engineering, Kyushu University

Matsumoto, Hikaru

Department of Chemical Engineering, Kyushu University

Nagao, Masanori

Department of Chemical Engineering, Kyushu University

Hironaka, Shuji

Department of Chemical Engineering, Kyushu University

他

<https://hdl.handle.net/2324/7337522>

---

出版情報 : Polymer Journal. 56 (9), pp.865-872, 2024-06-06. Society of Polymer Science, Japan (SPSJ)

バージョン :

権利関係 : This version of the article has been accepted for publication, after peer review (when applicable) and is subject to Springer Nature' s AM terms of use, but is not the Version of Record and does not reflect post-acceptance improvements, or any corrections. The Version of Record is available online at: <http://dx.doi.org/10.1038/s41428-024-00923-8>.



## Original Article

# The development of Pd immobilized porous polymer catalysts by the application of Bayesian optimization

Xincheng Zhou,<sup>1</sup> Hikaru Matsumoto,<sup>1</sup> Masanori Nagao,<sup>1</sup> Shuji Hironaka,<sup>1</sup> and Yoshiko Miura<sup>1\*</sup>

<sup>1</sup>Department of Chemical Engineering, Kyushu University, 744 Motooka, Nishi-ku, Fukuoka 819-0395, Japan

## Correspondence

**\*\***Yoshiko Miura, Kyushu University, 744 Motooka, Nishi-ku, Fukuoka 819-0395, Japan

Email: miuray@chem-eng.kyushu-u.ac.jp

**Running Head:** Optimization of polymer immobilized catalysts by machine learning

## **Abstract**

This study presented the preparation of a Pd-polymeric porous immobilized catalyst for Suzuki-Miyaura coupling reactions, employing Bayesian optimization method to optimize the catalyst. This research represented the first attempt to utilize machine learning for the optimization of polymer-immobilized catalysts, which provided a novel perspective on utilizing machine learning for the optimization of complex materials.

**Key Words:** Suzuki-Miyaura coupling / Polymer immobilized catalyst / Porous polymer/  
Machine learning / Bayesian optimization

## Introduction

In the past 30 years, transition metal-catalyzed reactions have found widespread use in organic synthesis.[1] Especially, cross-coupling, oxidation, addition, and metathesis reactions have been reported with excellent yields, selectivities, and functional group tolerance are employed for preparation of compound library and large-scale pharmaceutical production.[2] Suzuki-Miyaura coupling reactions are powerful tools for formation of carbon-carbon bonds because of mild reaction conditions, and easy separation of boron-containing by-products.[3] It is well known that phosphines are representative ligands for the Suzuki-Miyaura coupling reactions and their reactivities and selectivities can be adjusted by tuning the steric and/or electronic properties.[4]

In recent years, there has been growing interest in solid-supported catalysts for their insolubility in the reaction solution, facilitating easy separation and recycling from a green chemistry perspective.[5] Generally, the catalytic efficiencies of the supported catalysts are lower than those of homogeneous counterparts, mainly due to the limitations of mass transfer in the solid phase of the supported catalysts. To improve mass transfer in the supported catalysts, the fabrication of porous morphology on the support material is beneficial. Ma et al. achieved excellent reactivity and alkene selectivity in the semihydrogenation of terminal alkynes using Pd-immobilized porous polymer catalyst.[6] Due to easy preparation and high chemical stability, transition metal catalysts supported on porous polystyrene have been developed.[7] Matsumoto et al. developed a porous polystyrene monolith supporting phosphine-Pd complexes in Suzuki-Miyaura coupling, finding that large surface area and high existence ratio of mono-ligated phosphine-Pd complex improved catalytic efficiency. Particularly, the cross-

linking degree of the polystyrene significantly influenced the coordination behavior of phosphine-Pd complexes.[8] In order to achieve the highest activity for these polymer catalysts, a significant number of trial-and-error experiments are required. This process consumes a substantial amount of time and experimental resources. Optimizing catalysts manually through human effort is challenging due to the extensive experimental workload and associated costs. Therefore, automated learning and optimization based on existing data would enable substantial cost savings.

Machine learning is an information science that elucidates rules based on data and predicts properties.[9] With the remarkable development of the methodologies of machine learning in recent years, its applications in materials science have increased.[10] The application of machine learning in the field of polymers has gradually gained attention and made significant strides over the past five years, primarily due to the inherent complexity of polymers, the lack of appropriate descriptors, and the absence of extensive publicly available databases.[11] However, machine learning in the optimization of immobilized catalysts on synthetic polymers has not been reported yet. The complexity of the material's preparation makes it challenging to gather a large amount of data manually for building a machine learning model.

Herein, we first report a computer-guided and systematic approach to optimize polymer-supported catalyst in transition metal catalysis (Figure 1). As a machine learning method, we adopted a Bayesian optimization, which leverage existing predictive models to suggest the next sampling point and enable a faster convergence to the desired maximum value. Bayesian optimization samples points based on proposals given by an acquisition function, which balances exploration and exploitation to efficiently find the global maximum.[12] Applying

Gaussian processes as surrogate models in Bayesian optimization is advantageous for quantifying uncertainty in the exploration process and can achieve predictions of reaction yields. Consequently, Bayesian optimization achieves optimization goals with a minimal amount of experimental data.[13] In fact, researchers have applied Bayesian optimization to catalytic reactions,[14][15] and catalyst materials.[16][17] In this report, porous polystyrene monoliths supporting phosphine ligand with different cross-linking density and porous structure were synthesized varying polymerization conditions. The monoliths were obtained as self-standing materials during the polymerization-induced phase separation in a porogenic solvent (toluene/1-decanol).[8] The cross-linker and porogen contents were selected as independent variables, which influence the morphology and properties of pores. Additionally, the cross-linking monomer also impacts the coordination state. Therefore, selecting divinylbenzene (DVB) and 1-decanol contents as variables was appropriate. Turnover frequency (TOF) was selected as target variable for modelling using machine learning. Through Bayesian optimization of the dataset using Gaussian process, the points with predicted maximum TOFs were proposed and evaluated experimentally. This experimental validation and iterative machine learning cycles contribute to the gradual improvement of catalytic activity. This methodology smartly combines experimentation and intelligent data-driven optimization for enhanced catalyst performance.

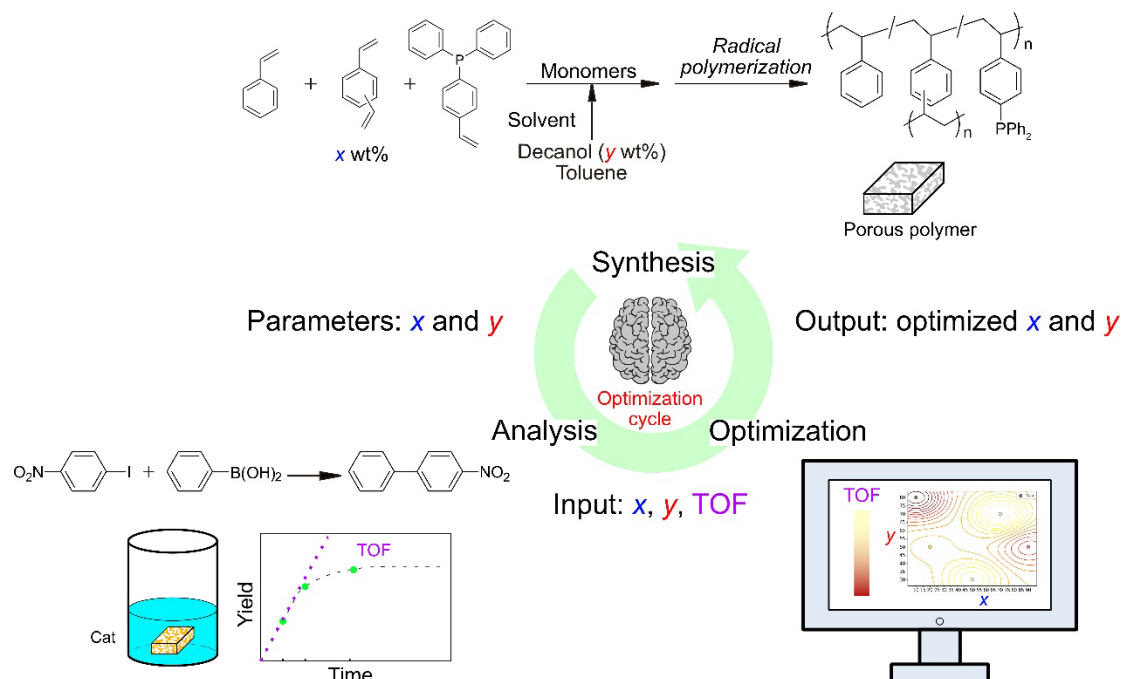


**Figure 1.** Workflow of machine-learning-guided optimization of Pd immobilized porous polymer catalysts. The monolith polymerization step involved two independent variables, namely the DVB content ( $x$ ) and 1-decanol content ( $y$ ) to maximize TOF as target variable in Suzuki-Miyaura coupling reaction. Bayesian optimization was applied for predictive modelling, and the optimized conditions were experimentally validated in subsequent iterations.

## Experimental

### Materials

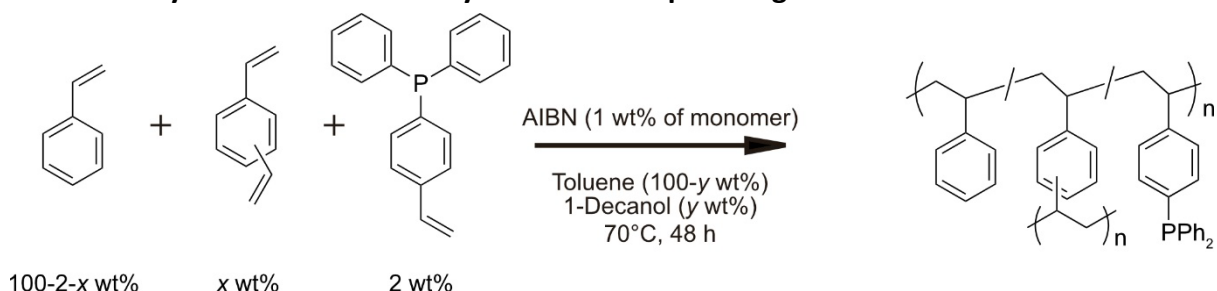
Water with a conductivity of 18.2 M $\Omega$  cm (Milli-Q, Millipore Co., Bedford, MA, USA) was used in all experiments. Styrene (St, >99% GC purity, stabilized with 4-*t*-butylcatechol, Tokyo Chemical Industry Co., Ltd., Tokyo, Japan) and DVB (*m*- and *p*- mixture, contains ethylvinylbenzene, diethylbenzene, stabilized with TBC, Tokyo Chemical Industry Co., Ltd.,

Tokyo, Japan) were purified using basic alumina column.[19] 2,2'-Azobis(isobutyronitrile) (AIBN, FUJIFILM Wako Pure Chemical Corporation), 4-(diphenylphosphino) styrene (VPP<sub>3</sub>, 97%, Sigma-Aldrich), bis(benzonitrile)palladium(II) dichloride (Pd(II), >98.0%, Tokyo Chemical Industry Co., Ltd., Tokyo, Japan), 1-decanol (99%, Tokyo Chemical Industry Co., Ltd., Tokyo, Japan), toluene (99.5%, FUJIFILM Wako Pure Chemical Corporation), tetrabutylammonium hydroxide (TBAOH, 10% in methanol, Tokyo Chemical Industry Co., Ltd., Tokyo, Japan), phenylboronic acid (contains varying amounts of anhydride, Tokyo Chemical Industry Co., Ltd., Tokyo, Japan), 1-iodo-4-nitrobenzene (>99%, Tokyo Chemical Industry Co., Ltd., Tokyo, Japan), 1-bromo-4-nitrobenzene (>99%, Tokyo Chemical Industry Co., Ltd., Tokyo, Japan), nitrobenzene (NO<sub>2</sub>Ph, min 99.5%, Wako Pure Chemical Industries, Ltd., Osaka, Japan). 4-chloronitrobenzene (>98%, Tokyo Chemical Industry Co., Ltd., Tokyo, Japan), tetrahydrofuran (THF, Super Dehydrated, with Stabilizer, Wako Pure Chemical Industries, Ltd., Osaka, Japan).



## Synthesis of monolith[8]

### Scheme 1. Synthesis of Porous Polymer with Phosphine Ligand<sup>a</sup>

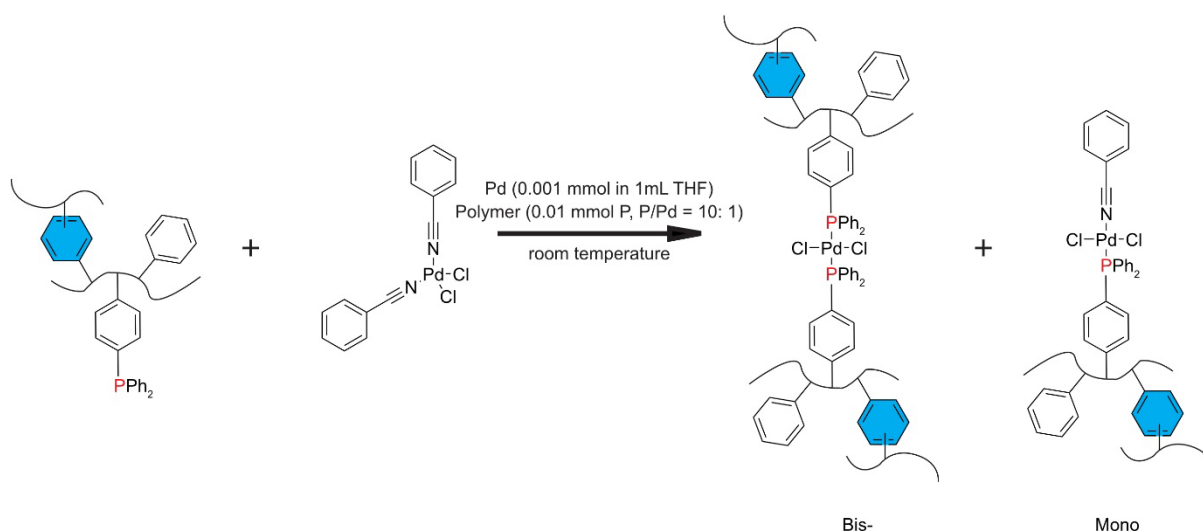


<sup>a</sup>Conditions: VPP<sub>3</sub> (2 wt% of monomer), DVB (x wt% of monomer), St (100 – x – 2 wt% of monomer), 1-decanol (y wt% of solvent), toluene content (100 – y wt% of solvent), AIBN (1 wt% of monomer). Total monomer conc.: 40 wt%, 70°C, 48h.

The monolithic porous polystyrene was prepared by the bulk copolymerization of VPP<sub>3</sub> (2 wt%), DVB (x wt%) and St (100 – x – 2 wt%) in a porogenic solvent. Monomers were dissolved in a mixture of 1-decanol (100 – y wt%) and toluene (y wt%) followed by addition of AIBN (1 wt% with respect to monomers) to give a monomer solution (1 g, 40 wt%) (Scheme 1). The monomer solution was prepared in a glass vial. After degassing via three freeze-pump-thaw cycles, the vial was charged with N<sub>2</sub> and subsequently sealed with a screw cap. Carefully crushing the vial, the resulting polymer was cut into ~5 mm small blocks and washed by immersion in anhydrous THF for more than 1 day with THF changing 3 times. The monoliths were dried in vacuo at room temperature overnight. The internal structures of the dried monoliths were observed using FE-SEM.

## Pd coordination

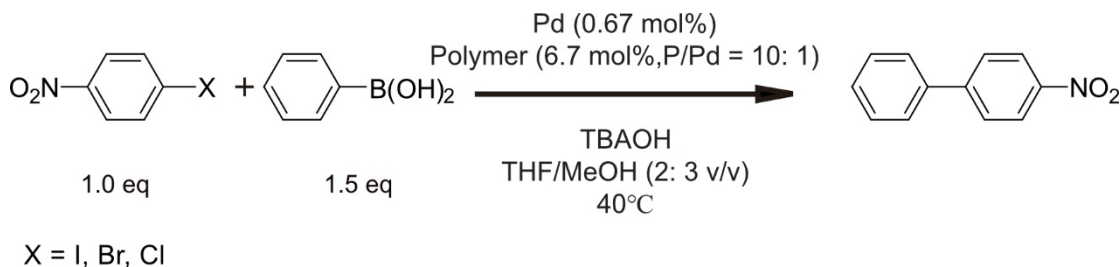
### Scheme 2. Ligand Exchange Reaction of Pd(II)



In a glove box, 2.3 mg of  $[\text{PdCl}_2(\text{PhCN})_2]$  (0.006 mmol) was dissolved in anhydrous THF (6 mL). Subsequently, 1 mL of the Pd solution (0.001 mmol Pd) was added to dried and cubic monolith (144 mg, 0.01 mmol of P, P/Pd 10: 1) in a glass vial. The mixture was placed at room temperature for over 4 h while the THF-swollen monolith turned into yellow. Removed from the glove box, the Pd loaded monolith was washed with anhydrous THF (2 mL). The absorbance of the reaction mixture was measured using ultraviolet-visible (UV-Vis) at 440 nm to confirm the complete coordination of Pd(II) (Scheme 2).

## Suzuki-Miyaura coupling reaction using Pd-loaded monolith

Scheme 3. Pd-Catalyzed Suzuki-Miyaura Coupling Reaction of *p*-halogenated nitrobenzenes



The Suzuki-Miyaura coupling reaction between *p*-halogenated nitrobenzenes and phenylboronic acid was conducted in the presence of TBAOH in a THF/MeOH mixture. Initially, a THF reaction mixture was prepared in a glove box: *p*-halogenated nitrobenzenes (0.25 mmol), phenylboronic acid (45.5 mg, 0.375 mmol), and  $\text{NO}_2\text{Ph}$  (20  $\mu\text{L}$ , used as an internal substance) were dissolved in anhydrous THF (5 mL). Subsequently, a portion of the substrate solution (3 mL, containing 1-bromo-4-nitrobenzene 0.15 mmol, 1 eq; phenylboronic acid 0.225 mmol, 1.5 eq;  $\text{NO}_2\text{Ph}$  12  $\mu\text{L}$ ) was added to a glass vial containing Pd-loaded monolith (Pd 0.001 mmol, 0.67 mol%, P/Pd = 10:1). Next, TBAOH (10% in MeOH, 4.5 mL, 0.45 mmol, 3 eq) was added to the reaction mixture, and the glass vial was purged with nitrogen. The reaction was initiated in a water bath at 40°C and a small aliquot was collected using a syringe in the context of varying reaction times, then analyzed using HPLC to determine a yield of 4-nitrobiphenyl (Scheme 3).

## Results and Discussion

### Preparation and characterization of porous polymer immobilized catalysts

Our research commenced with the synthesis of porous polymer monoliths containing phosphine ligands. The radical polymerization of St, DVB, and VPP<sub>3</sub> in a mixed solution of toluene and 1-decanol gave a monolithic and porous structure due to polymerization-induced phase separation.[8] The obtained monoliths were cut into pieces, washed by immersion in anhydrous THF, and dried under vacuum. SEM images confirmed that the monolith exhibits a porous structure, with pore sizes ranging between macro- and mesopores (5-600 nm, Figure 2a and Figure S1). Through the mercury intrusion experiment, the pore sizes and distribution of each monolith were determined, revealing that the pore sizes ranged from 5 to 263 nm (Figure 2b, Figure S5 and Table S1). The heterogeneous pore size distribution may be related to the exothermic nature during the polymerization.[18] Catalyst entry 7, exhibiting a characteristic of multiple pore size distributions, thus suggests no evidence indicating that the heterogeneous pore size distribution would adversely affect the catalyst activity. The results from solid-state NMR measurements confirmed that the polymerized monolith contains free P (Figure 2c and Figure S6). In the NMR spectrum, two peaks were observed at chemical shifts of 23 ppm and -6 ppm, respectively, indicating the presence of oxidized P and free P.[8] The dried monolith was immersed in a THF solution of [PdCl<sub>2</sub>(PhCN)<sub>2</sub>] (P/Pd = 10:1) for complexation between polymer-supported phosphine and Pd. After 4 h, the absence of free Pd in the solution was confirmed using UV-Vis spectroscopy, indicating successful immobilization of Pd on the monoliths. The solid state <sup>31</sup>P NMR of the monoliths after Pd loading showed a peak in the

vicinity of 24 ppm, accompanied by the peak area of free P decreasing (Figure 2c and Figure S6). It was suggested that Pd coordination exclusively yields P-Pd bis-complexes (24 ppm) rather than mono-coordinated Pd.[8] This result demonstrated the successful immobilization of Pd-P complexes onto polystyrene with varying polymer compositions and porous structures.

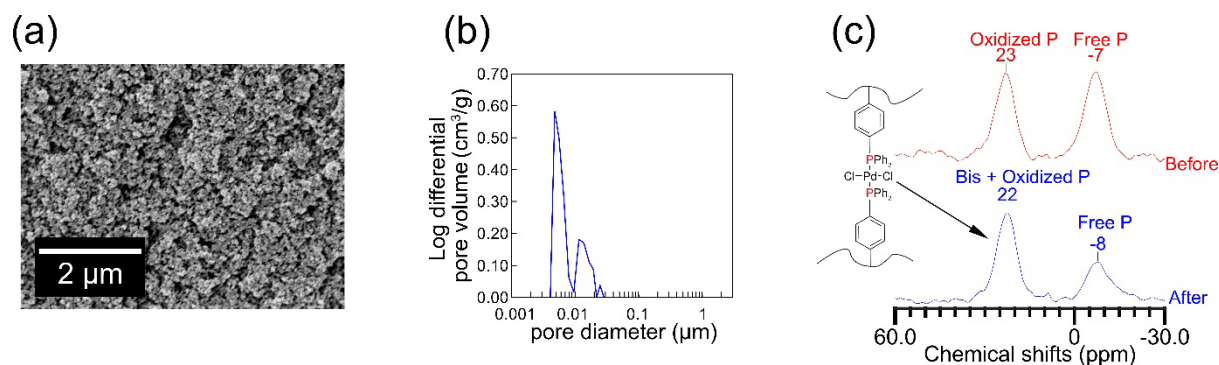


**Figure 2.** The properties of polymer 7. (a) SEM image, (b) pore size distributions, (c)  $^{31}\text{P}$  CP/MAS NMR spectra before and after catalytic reaction.

## Catalytic Activity for Suzuki-Miyaura coupling Reaction and Bayesian Optimization

The catalytic activities of the Pd-immobilized monoliths were evaluated in Suzuki-Miyaura coupling reactions. The initial dataset included 5 different compositions of monoliths, where the DVB and 1-decanol contents were varied (polymer 1–5, entries 1–5, Table 1). The Suzuki-Miyaura coupling reaction between 1-iodo-4-nitrobenzene and phenylboronic acid was conducted at 40°C. Small aliquots of the reaction mixture were collected at 5 min and analyzed using high performance liquid chromatography (HPLC), to determine the TOF of the catalyst

as a target variable (entries 1–5, Table 1). From time-yield profile of the catalytic reactions, all the reactions were completed within 20 min (entries 1–5, Figure S4).

**Table 1. The Activity of Suzuki-Miyaura Coupling Reactions Catalyzed by Pd Immobilized Porous Polymer Catalysts<sup>a</sup>**

Entry	Polymer	Data type in machine learning	DVB content (x) [wt%]	1-Decanol content (y) [wt%]	X	Yield (%)	TOF (min <sup>-1</sup> )
1	1	Initial	10	80	I	41	12.3
2	2	Initial	50	30	I	57	17.1
3	3	Initial	90	50	I	47	14.1
4	4	Initial	70	70	I	59	17.7
5	5	Initial	20	50	I	53	15.9
6	6	1 <sup>st</sup> run	61	66	I	69	20.7
7	7	1 <sup>st</sup> run	39	24	I	81	24.3
8	8	2 <sup>nd</sup> run	33	20	I	11	3.3
9	9	2 <sup>nd</sup> run	53	60	I	19	5.7
10	7		39	24	Br	78 <sup>b</sup>	1.5 <sup>d</sup>
11	7		39	24	Cl	3 <sup>c</sup>	n.d.

<sup>a</sup>Conditions: aryl halide (0.15 mmol, 1 eq), phenylboronic acid (0.225 mmol, 1.5 eq), tetrabutylammonium hydroxide (TBAOH, 10% in MeOH, 0.45 mmol, 3 eq), THF/MeOH (2:3 v/v), catalyst (0.67 mol% Pd, P/Pd = 10:1), 40°C, 5 min. <sup>b</sup>At 140 min. <sup>c</sup>At 150 min. <sup>d</sup>Calculated from 10 to 60 min.

Machine learning was employed using GPy[20] model in Python to conduct Bayesian optimization of the polymerization conditions (DVB content (x) and 1-decanol content (y)) for higher catalytic activities. Gaussian kernel functions and Gaussian processes were utilized

during the optimization process. The Bayesian optimization was acted during four steps: (i) the gaussian process was used as a surrogate model, and the model was established with the initial data, (ii) the predicted average and confidence were acquired from the model, and the next experimental point was given based on the maximized acquisition function, which was upper confidence bound (UCB) in the present study, (iii) perform the experiment with selected next sampling point, and (iv) add the new experiment points and continue optimization for updating the model. The initial Bayesian optimization was conducted with 5 initial data (entries 1–5, Table 1), and contour map of the model was illustrated (Figure 3a). Color gradient represents the TOFs, with red color indicating higher values and blue color indicating lower values. This visualization effectively represents the machine learning model utilizing Bayesian optimization of two variables. Subsequently, the contour map was sliced along both the horizontal and vertical axes at the predicted points corresponding to higher TOFs (red regions), resulting in two different sectional views (Figure 3b–e). Due to the separation of the two red regions in the initial contour map, we generated four sectional views corresponding to each red region. In the sectional view, dark blue line and light blue area indicate a predicted mean and a 25 to 75% prediction confidence interval. To determine the predicted maximum TOFs, we selected the upper limit of the confidence interval as the maximum point. This method of sampling points based on proposals can be described using the UCB acquisition function. It was judged based on observing the upper limit of the 50% confidence interval. The maximum point in the upper red region corresponded to DVB and 1-decanol contents of 61 and 66 wt%, respectively (Figure 3b and c). Likewise, in the lower red region, the optimized DVB and 1-decanol contents were 39 and 24 wt%, respectively (Figure 3c and d).

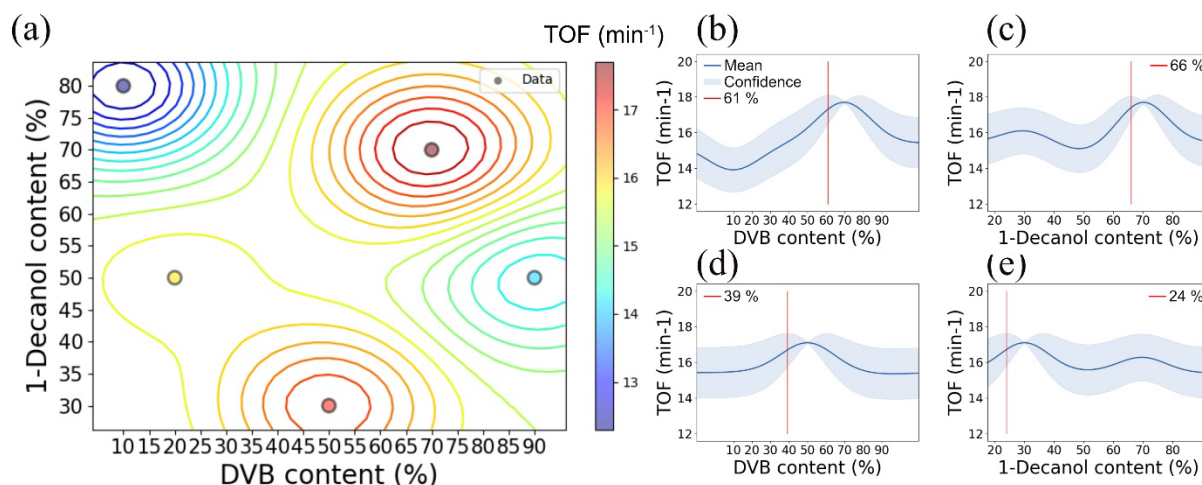


**Figure 3.** The 1st Gaussian process regression GPy for entries 1-5 in Table 1. (a) Estimated yield, (b) predicted yield for DVB content in the red ring above in Figure 3a, (c) predicted yield for 1-decanol content in the red ring above in Figure 3a, (d) predicted yield for DVB content in the red ring below in Figure 3a and (e) predicted yield for 1-decanol content in the red ring below in Figure 3a.

According to the Bayesian optimization, monoliths were prepared under the optimal polymerization conditions (polymer 6 and 7, entries 6 and 7, Table 1), and evaluated for their TOFs in the Pd-catalyzed cross-coupling reactions (entries 6 and 7, Table 1). Amazingly, the significant improvement of catalytic activities was observed for the polymer 6 and 7 to give TOFs of 20.7 and 24.3 min<sup>-1</sup>, respectively (entries 6 and 7), compared with those of initial dataset (TOFs of 12.3–17.7 min<sup>-1</sup>, entries 1–5, Table 1).

These data (entries 1-7) were added to the dataset and subjected to a 2nd-round machine learning using Bayesian optimization to obtain the polymer compositions (polymer 8 and 9,



entries 8 and 9, Table 1) that would generate higher activity (Figure S2). Unfortunately, these catalysts yielded smaller TOF values (3.3 and 5.7 min<sup>-1</sup>, entries 8 and 9, Table 1) and longer reaction times were required to complete the catalytic reaction (entries 8 and 9, Figure S3). Since no improvement was obtained in the second optimization, we determined that the entry 7 with the highest TOF (TOF = 24.3 min<sup>-1</sup>, entry 7, Table 1) was the best catalyst, considering the research goal of reducing the number of experiments. This outcome demonstrated the success of Bayesian optimization in polymeric immobilized catalysts, establishing a direct correlation between the variables involved in polymer preparation and the desired final properties, while disregarding intermediate complex variables. This simplification of the optimization process led to successful development of polymer-supported catalysts with minimal time and experimental costs.

Bayesian optimization has been applied in the polymer field, especially in optimizing polymerization processes and enhancing polymer performance. In processes for polymeric materials, the shape of fibers,[21] producibility,[22] and polymerization kinetics[23] have been optimized by Bayesian optimization. On the other hand, designing and improving the sophisticated functions of the polymers are tedious and time consuming. In this sense, several functional polymers have been improved using Bayesian optimization for electrically insulating performance,[24] water permeability and selectivity,[25] mechanical/thermal properties,[26] antimicrobial efficiency,[27] and abrasion tolerance.[28] In this research, we investigated the porous polymer monolith with diverse structure and morphologies for high catalytic performance. Thus far, there has been a lack of research applying Bayesian optimization to polymer catalysts. This study represents the first attempt to apply Bayesian

optimization to the composition of polymers, successfully optimizing porous heterogeneous polymer materials.

## **Characterization of Pd Nanoparticle Formation during Catalytic Reaction Progression**

Before and after the catalytic reaction, the monolith was analyzed using scanning transmission electron microscopy (STEM) and energy-dispersive X-ray spectroscopy (EDX). It can be inferred that before catalytic reactions, Pd were atomically dispersed on the monoliths, without forming nanoparticles (Figure 4a). After catalytic reaction, it was obvious that Pd nanoparticles formed (Figure 2a and b). The size distributions of the Pd were similar (4-15 nm) among the best and the worst monolith catalysts (entries 7 and 8, Table 1).

The relationship between the porous properties and reaction activities was evaluated and analyzed (Table S3), however, there was no clear evidence to establish those correlation (see ESI for the detail). Since all Pd species on the monoliths were bis-P-ligated, the coordination state was not a factor to variations in catalytic activity. According to the STEM (Figures 4b, c, S7, and S8), there was minimal difference in the particle size of Pd among the monoliths. It was found that the formation and growth of nanoparticles are unrelated to their catalytic activities. Therefore, a hypothesis was proposed that the process of Pd aggregation to form particles was correlated with the extent of catalytic reaction. Since both the best and worst monoliths showed the same TON, the resulting particle sizes were roughly similar. It could be

concluded that the aggregation of Pd particles was a consequence of the catalytic reaction, rather than the cause of the difference in reaction activity.

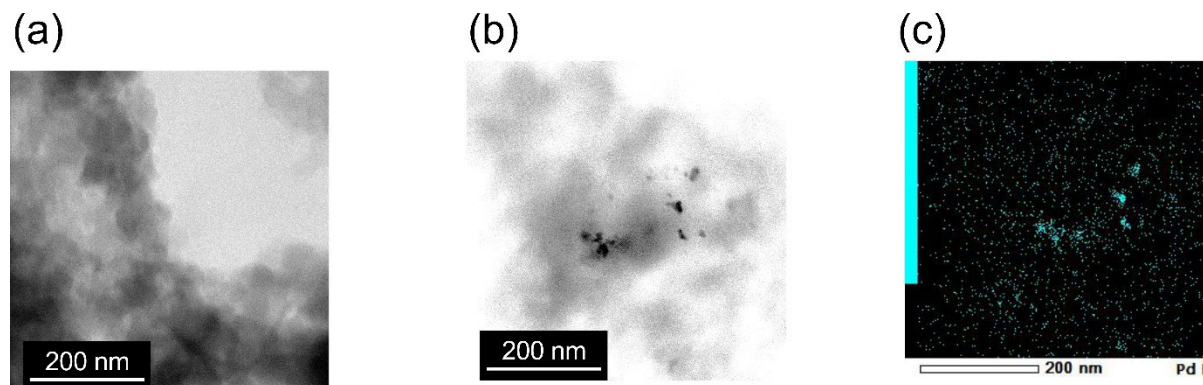


**Figure 4.** The properties of polymer 7. (a) bright-field STEM image after Pd coordination and (b) catalytic reaction, and (c) EDX mapping for Pd.

### Performance of this Catalyst with Various Reactants

We applied the best catalyst to the Suzuki-Miyaura coupling reactions of different *p*-halogenated nitrobenzenes ( $X = \text{Br}$  or  $\text{Cl}$ ). From the reaction kinetic curves of the catalytic reactions revealed that the yield of the 4-nitrobiphenyl (78% at 140 min) and TOF ( $1.5 \text{ min}^{-1}$ ) were moderate using 1-bromo-4-nitrobenzene (entry 10, Table 1). On the other hand, 4-chloronitrobenzene showed lower reactivity (3% at 150 min) (entry 11, Table 1). The reactivity of aromatic halides followed the trend  $\text{I} > \text{Br} > \text{Cl}$ , as reported in the literature. It was reported that aromatic chlorides did not undergo Suzuki-Miyaura coupling reactions, and Suzuki-Miyaura coupling reactions involving aromatic bromides required higher reaction temperatures and longer reaction times compared to aromatic iodides.[29] The catalyst employed in this

study facilitated Suzuki-Miyaura coupling reactions for both aromatic iodides and aromatic bromides. Moreover, the reaction conditions were relatively mild, and the reaction proceeded at a fast rate.

## **Conclusions**

In summary, our research utilized the machine learning method of Bayesian optimization to optimize the composition of polymeric porous immobilized catalysts and the composition of the porogenic agents. Following the optimization, the catalyst exhibited enhanced reaction activity (TOF increased from 17.7 to 24.3 min<sup>-1</sup>). This paper presents an approach to optimize polymeric catalysts using machine learning, establishing a direct connection between the dependent and independent variables without considering the influence of intermediate variables. Moreover, the application of Gaussian process-based Bayesian optimization offered the advantage of optimization with minimal data, significantly simplifying the originally complex optimization process in catalyst chemistry and materials science.

## **Compliance with Ethical Standards**

The authors declare that they have no conflict of interest.

## **Acknowledgements**

X. Zhou, H. Matsumoto and Y. Miura designed the experiments. X. Zhou performed the experiments. X. Zhou and H. Matsumoto wrote the manuscript. M. Nagao made contributions to the discussions during the work. S. Hironaka provided guidance for machine learning. All authors have given approval to the final version of the manuscript.

## References

- [1] Ojima I, Tzamarioudaki M, Li Z, Donovan RJ. Transition Metal-Catalyzed Carbocyclizations in Organic Synthesis. *Chem. Rev.* 1996; 96; 635-662.
- [2] Magano J, Dunetz JR. Large-Scale Applications of Transition Metal-Catalyzed Couplings for the Synthesis of Pharmaceuticals. *Chem. Rev.* 2011; 111; 2177-2250.
- [3] Miyaura N, Suzuki A, Stereoselective synthesis of arylated (E)-alkenes by the reaction of alk-1-enylboranes with aryl halides in the presence of palladium catalyst. *J. Chem. Soc. Chem. Commun.* 1979; 866-867.
- [4] Martin R, Buchwald SL. Palladium-Catalyzed Suzuki–Miyaura Cross-Coupling Reactions Employing Dialkylbiaryl Phosphine Ligands. *Acc. Chem. Res.* 2008; 41; 1461-1473.
- [5] Lu J, Toy PH. Organic Polymer Supports for Synthesis and for Reagent and Catalyst Immobilization. *Chem. Rev.* 2009; 109; 815-838.
- [6] Liu J, Wang N, Liu J, Li M, Xu Y, Wang C, Wang Y, Zheng H, Ma L. The Immobilization of Pd(II) on Porous Organic Polymers for Semihydrogenation of Terminal Alkynes. *ACS Appl. Mater. Interfaces.* 2020; 12; 51428-51436.
- [7] Sundell MJ, Pajunen EO, Hormi OEO, Nasman JH. Synthesis and Use as a Catalyst Support of Porous Polystyrene with Bis(phosphonic acid) -Functionalized Surfaces. *Chem. Mater.* 1993; 5; 372-376.
- [8] Matsumoto H, Hoshino Y, Iwai T, Sawamura M, Miura Y. Polystyrene-Supported PPh<sub>3</sub> in Monolithic Porous Material: Effect of Cross-Linking Degree on Coordination Mode and Catalytic Activity in Pd-Catalyzed C–C Cross-Coupling of Aryl Chlorides. *ChemCatChem.* 2020; 12; 4034-4037.

- [9] Williams WL, Zeng L, Gensch T, Sigman MS, Doyle AG, Anslyn EV. The Evolution of Data-Driven Modeling in Organic Chemistry. *ACS Cent. Sci.* 2021; 7; 1622-1637.
- [10] Wang AYT, Murdock RJ, Kauwe SK, Oliynyk AO, Gurlo A, Brgoch J, Persson KA, Sparks TD. Machine Learning for Materials Scientists: An Introductory Guide toward Best Practices. *Chem. Mater.* 2020; 32; 4954-4965.
- [11] Martin TB, Audus DJ. Emerging Trends in Machine Learning: A Polymer Perspective. *ACS Polym. Au.* 2023; 3; 239-258.
- [12] Shahriari B, Swersky K, Wang Z, Adams RP, Freitas N. Taking the Human Out of the Loop: A Review of Bayesian Optimization. *P. IEEE.* 2016; 104; 148-175.
- [13] Rasmussen CE, Williams CKI. *Gaussian Processes for Machine Learning.* The MIT Press. Cambridge. MA. 2006.
- [14] Shields BJ, Stevens J, Li J, Parasram M, Damani F, Alvarado JIM, Janey JM, Adams RP, Doyle AG. Bayesian reaction optimization as a tool for chemical synthesis. *Nature.* 2021; 590; 89-96.
- [15] Kondo M, Wathsala HDP, Sako M, Hanatani Y, Ishikawa K, Hara S, Takaai T, Washio T, Takizawa S, Sasai H. Exploration of flow reaction conditions using machine-learning for enantioselective organocatalyzed Rauhut–Currier and [3+2] annulation sequence. *Chem. Commun.* 2020; 56; 1259-1262.
- [16] Wang X, Huang Y, Xie X, Liu Y, Huo Z, Lin M, Xin H, Tong R. Bayesian-optimization-assisted discovery of stereoselective aluminum complexes for ring-opening polymerization of racemic lactide. *Nat Commun.* 2023; 14; 3647.
- [17] Feng X, Gong X, Liu D, Li Y, Jiang Y, Zhang Y. Bayesian Optimization-guided Discovery

- of High-performance Methane Combustion Catalysts based on Multi-component PtPd@CeZrOx Core–Shell Nanospheres. *Angew. Chem. Int. Ed.* 2023; 62; e202313068.
- [18] Peters EC, Svec F, Frechet JMJ. Preparation of large-diameter “Molded” porous polymer monoliths and the control of pore structure homogeneity. *Chem. Mater.* 1997; 9; 1898–1902.
- [19] LeBlond CR, Andrews AT, Sun Y, Sowa JR. Activation of Aryl Chlorides for Suzuki Cross-Coupling by Ligandless, Heterogeneous Palladium. *Org. Lett.* 2001; 3; 1555-1557.
- [20] The GPy authors. GPy: A Gaussian process framework in Python. <http://github.com/SheffieldML/Gpy>.
- [21] Li C, Leal DRC, Rana S, Gupta S, Sutti A, Greenhill S, Slezak T, Height M, Venkatesh S. Rapid Bayesian optimization for synthesis of short polymer fiber materials. *Sci. Rep.* 2017; 7; 5683.
- [22] Wang A, Ye H, Yang Y, Dong H. Bayesian optimization of HDPE copolymerization process based on polymer product-process integration. *Polymer.* 2024; 292; 126554.
- [23] Fan S, Zhang X, Hong X, Liao Z, Chen Y, Ren C, Yang Y, Wang J, Yang Y. Kinetic Parameter Estimation of the Polyethylene Process by Bayesian Optimization. *Ind. Eng. Chem. Res.* 2024 (*in press*).
- [24] Iyer A, Zhang Y, Prasad A, Gupta P, Tao S, Wang Y, Prabhune P, Schadler LS, Brinson LC, Chen W. Data centric nanocomposites design via mixed-variable Bayesian optimization. *Mol. Syst. Des. Eng.* 2020; 5; 1376-1390.
- [25] Gao H, Zhong S, Zhang W, Igou T, Berger E, Reid E, Zhao Y, Lambeth D, Gan L, Afolabi MA, Tong Z, Lan G, Chen Y. Revolutionizing Membrane Design Using Machine

- Learning-Bayesian Optimization. *Environ. Sci. Technol.* 2022; 56; 2572–2581.
- [26] Albuquerque RQ, Rothenhäusler F, Gröbel P, Ruckdäschel H. Multi-Objective Optimization of Sustainable Epoxy Resin Systems through Bayesian Optimization and Machine Learning. *ACS Appl. Eng. Mater.* 2023; 1; 3298–3308.
- [27] Judzewitsch PR, Corrigan N, Trujillo F, Xu J, Moad G, Hawker CJ, Wong EHH, Boyer C. High-Throughput Process for the Discovery of Antimicrobial Polymers and Their Upscaled Production via Flow Polymerization. *Macromolecules.* 2020; 53; 631–639.
- [28] Nahvi A, Sadoughi MK, Arabzadeh A, Sassani A, Hu C, Ceylan H, Kim S. Multi-objective Bayesian optimization of super hydrophobic coatings on asphalt concrete surfaces. *J. Comput. Des. Eng.* 2019; 6; 693-704.
- [29] Matsumoto H, Inaba S, Rieke RD, Activated metallic nickel as a reagent for the dehalogenative coupling of halobenzenes. *J. Org. Chem.* 1983; 48; 840-843.